# Multispecies Purification of Testicular Germ Cells[1]

Ana C. Lima,[3,4,5,6,7] Min Jung,[3,4] Jannette Rusch,[4] Abul Usmani,[4] Alexandra M. Lopes,[6,7] and Donald F. Conrad[2,8]

[4]*Department of Genetics, Washington University School of Medicine, St. Louis, Missouri*
[5]*Graduate Program in Areas of Basic and Applied Biology (GABBA), Abel Salazar Institute of Biomedical Sciences, University of Porto, Porto, Portugal*
[6]*Instituto de Investigação e Inovação em Saúde, Universidade do Porto, Porto, Portugal*
[7]*Instituto de Patologia e Imunologia Molecular da Universidade do Porto, Porto, Portugal–IPATIMUP, Porto, Portugal*
[8]*Department of Pathology & Immunology, Washington University School of Medicine, St. Louis, Missouri*

## ABSTRACT

Advanced methods of cellular purification are required to apply genome technology to the study of spermatogenesis. One approach, based on flow cytometry of murine testicular cells stained with Hoechst-33342 (Ho-FACS), has been extensively optimized and currently allows the isolation of nine germ cell types. This staining technique is straightforward to implement, is highly effective at purifying specific germ cell types, and yields sufficient cell numbers for high-throughput studies. Ho-FACS is a technique that does not require species-specific markers, but whose applicability to other species is largely unexplored. We hypothesized that, because of the similar cell physiology of spermatogenesis across mammals, Ho-FACS could be used to produce highly purified subpopulations of germ cells in mammals other than mouse. To test this hypothesis, we applied Ho-FACS to four mammalian species that are widely used in testis research: *Rattus norvegicus*, *Cavia porcellus*, *Canis familiaris*, and *Sus scrofa domesticus*. We successfully isolated four germ cell populations from these species with average purity of 79% for spermatocytes, 90% for spermatids, and 66% for spermatogonia. Additionally, we compare the performance of mechanical and chemical dissociation for each species, and propose an optimized gating strategy to better discriminate round and elongating spermatids in the mouse, which can potentially be applied to other species. Our work indicates that spermatogenesis may be uniquely accessible among mammalian developmental systems, as a single set of reagents may be sufficient to isolate germ cell populations from many different mammalian species, opening new avenues in the fields of development and male reproductive biology.

## INTRODUCTION

Spermatogenesis is a complex developmental process in which early spermatogonial stem cells differentiate into spermatozoa in the seminiferous tubules of the testes. The study of this fascinating process has produced critical insights into stem cell biology [1], developmental gene regulation [2], adaptive evolution [3] and fertility [4]. With over 30 different distinct cell types in the vertebrate testis, there is exceptional diversity in the expression profiles of cells within a single individual, which can become confounding when studying expression differences among individuals or developmental stages [5]. This has compelled researchers to develop methods for effective male germ cell enrichment and isolation, such as StaPut velocity sedimentation, elutriation, magnetic-activated cell sorting (MACS), whole testis collection during first wave of spermatogenesis, and fluorescence-activated cell sorting (FACS) with Hoechst-33342 (Hoechst).

StaPut and elutriation are fairly efficient techniques that allow separation of different germ cells based on their size and density. When applied to mice, StaPut yields about $10^8$ cells/population from 22 testes with 90% purity, whereas approximately $10^7$ cells/population can be obtained by elutriation of two testes with 80%–95% purity rate [6, 7]. In both methods, the fractionation step that collects purified cells from different bovine serum albumin or Percoll gradients is labor intensive (3–4 h) and requires proficiency from practice as well as specific equipment. Also, both techniques are unsuitable for detailed molecular studies during meiosis as they can separate only one type of meiotic cell subpopulation at a time and fail to yield sufficient purity [8, 9]. MACS, which separates desired germ cell populations by conjugating the germ cells with a known surface marker antibody primed with magnetic beads, may circumvent this issue by performing purification in parallel with population-specific antibodies. However, only spermatogonia (Spg) and spermatids (Spd) are proven to have established surface markers for successful enrichment [6]. Furthermore, antibody-assisted purification has limitations in that it is necessary to develop species-specific reagents for each marker, and antibody-assisted purification typically does have the sensitivity to discriminate between cells at slightly different stages of a quantitative developmental process. Collecting mouse testis samples at specific days postpartum, timed for the first appearance of different germ cell types during the first

wave of spermatogenesis, is also used to enrich specific germ cell populations [10]. Given that the testis size is very small at those time points, and that samples comprise a mixture of all testicular cells, this approach is experimentally challenging and fails to detect intrinsic biological variations among individual cells. Importantly, evidence from different studies suggests that the first wave is regulated differently from adult spermatogenesis [10–12].

FACS of Hoechst-stained (Ho-FACS) murine male germ cells can discriminate nine germ cell types [8, 13–16]. Hoechst is a vital dye that binds preferentially to poly(d[AT]) sequences in the minor groove of DNA, with secondary binding taking place at higher ratios. These two DNA binding sites show varying binding energies and consequent spectrum shifts in relation to chromatin amount and structure [17, 18]. It has been proposed that this spectral shift could be used to discriminate between cells with similar DNA content but different chromatin properties [19–21]. Indeed, Ho-FACS of male germ cells exhibits a pattern that reflects changes in DNA content (blue fluorescence) and chromatin structure (red fluorescence) throughout spermatogenesis. In fact, red fluorescence shifts resulting from progressive chromatin decondensation during meiotic prophase allow the resolution of different meiotic subpopulations [13, 15]. Spermatogonial stem cells are an exception and represent a side population because of BCRP1-dependent dye efflux, which is switched off after the spermatogonial stages [13]. Therefore, measuring Hoechst intensity as a function of blue and red fluorescence is representative of three cellular properties: ploidy, chromatin structure/accessibility, and dye efflux caused by ABC transporter activity [13, 15, 22, 23]. With over 95% purity of sorted populations [15] and an average of $10^7$ cells/population from two testes in less than 2 h, this technique has proven highly efficient and less labor intensive. Although the actual FACS session requires specialized sorting equipment (ultraviolet [UV] laser) and a skilled operator, many research facilities provide cell-sorting services.

Recently, there is a growing interest in applying genomic technology to germ cells, especially in an evolutionary context [24, 25]. In that sense, purified cells can be used for numerous applications ranging from studying gene regulation to nucleosome mapping, epigenetics, development in germ cells, and many more [26–28]. To unravel the complexity of germ cells at a genomic level, researchers need an efficient and high-throughput purification technique that can be applied easily to many species. Given that Ho-FACS is not based on a species-specific molecular signature (e.g., an antigen), and that the cellular machinery for spermatogenesis is similar across all vertebrates, we hypothesized that separation of different germ cell types by Ho-FACS could be applied to other species. To test this hypothesis, we applied Ho-FACS to four species that are highly valued by the testis research community: *Rattus norvegicus* (rat), *Cavia porcellus* (guinea pig), *Canis familiaris* (dog), and *Sus scrofa domesticus* (miniature pig; hereafter mini pig).

Our results provide detailed descriptions on how Ho-FACS performs with an optimized gating strategy that includes a cell viability gate with propidium iodide (PI) staining and a DNA content gate at cell enrichment for four primary types of germ cells in each of the four species that we investigate. Each of our target spermatogenic germ cell types could be distinguished by Ho-FACS of the diploid (2C) mammalian species. We also demonstrate the use of a mechanical testis dissociation protocol in comparison to species-specific conditions for enzymatic dissociation, and present an optimized FACS gating strategy based on cell shape, size, and complexity to distinguish elongating Spd (eSpd) and round Spd (rSpd) in mouse. Collectively, we offer the first proof of principle that flow cytometry can be applied transversally across mammalian species to isolate Hoechst-stained male germ cells in different developmental stages.

## MATERIALS AND METHODS

### Animals

C57BL/6 male mice (Jackson Laboratory), Sprague Dawley male rats (Harlan Bioproducts), guinea pigs, and mini pigs were raised in animal facilities at Washington University in St. Louis. Dog testes were collected at Hillside Animal Hospital (St. Louis, MO) from animals scheduled for castration, and were transported to the lab on ice for immediate processing. Prior to surgery, dogs are routinely injected with lidocaine and bupivacaine to help with the recovery process. All testis samples were obtained from sexually mature animals (mice, 8–12 wk; rats, 70 days; dogs, 12–24 mo; guinea pigs, 3 mo; and mini pigs, 6 mo) and procedures were conducted in compliance with regulations of the Animal Studies Committee at Washington University in St. Louis.

### Collection and Processing of Testicular Tissue

Fresh testes from each species were decapsulated, rinsed in 1× PBS (#AM9625; Thermo Scientific), and cut to the size of mouse testis (approximately 1.5 × 0.7 cm). These tissue fragments were used without further processing for dissociation and FACS sorting or fixed for histology. For immunofluorescence, tissue was fixed in 4% paraformaldehyde (PFA; #15710; VWR) overnight at 4°C and washed with 70% ethanol at least three times. Testes sections used for hematoxylin-eosin (HE) staining were collected in modified Davidson solutions (24 h at room temperature with gentle rotation; #64133-50; Electron Microscopy Sciences), fixed in Bouin solution (24 h at room temperature with gentle rotation; #HT101128; Sigma), and washed with 70% ethanol until any remaining yellow color of Bouin fixative was completely removed.

### Immunofluorescence and HE Staining

Fixed testes samples were processed in an ethanol series and embedded in paraffin and 5-μm sections were cut. Slides were deparaffinized with xylene and rehydrated to PBS through sequential ethanol washes with decreasing alcohol concentrations. Standard HE staining was performed according to HE protocol adapted from Belinda Dana (Department of Ophthalmology, Washington University in St. Louis School of Medicine) with Hematoxylin 560 (#3801570; Surgipath) and 1% Alcoholic Eosin Y 515 (#3801615; Surgipath) for overall morphological evaluations. Immunofluorescence staining was performed after antigen retrieval (boiling in citric acid buffer for 20 min) and tissue permeabilization/blocking (0.5% Triton X-100 + 2% goat serum in 1× PBS for 1 h at room temperature). Primary (anti-P-H3[ser10]; #Ab5176; AbCam) and secondary (goat antirabbit ALF 633; #A21071; Life Technologies) antibodies were diluted (1:100 and 1:500 respectively) in antibody dilution buffer (1× PBS + 1% Tween 20 + 1% BSA) and incubated overnight at 4°C and 4 h at room temperature, respectively, in a humid chamber. After secondary antibody incubation, sections were stained with Hoechst (1:500; #H3570; Life Technologies), washed with 1× PBS, and mounted with ProLong Diamond Antifade Mountant (#P36961; Life Technologies). For comparative purposes with FACS-sorted germ cells, only Hoechst fluorescence is shown from these sections.

### Testis Dissociation and Hoechst Staining

Two different types of testicular dissociation protocols were used in this work: enzymatic and mechanical. The latter was performed using a Medimachine system (Cat. #340588; BD Biosciences) in line to the method previously described for rodents in [29]. A multispecies enzymatic dissociation protocol was designed based on the procedure described in [8] for mouse, as described below, and species-specific adjustments were made in terms of enzymes used, their relative concentrations, and incubation time and temperatures (see Supplemental Data; Supplemental Data are available online at www.biolreprod.org). Except for mini pig, whose species-specific adjustments were made according to [30], enzymatic dissociation conditions were adopted following the Worthington references for reproductive tissue dissociation [31].

*Enzymatic dissociation of testicular tissue (multispecies protocol).* Solutions (fresh; prior to testes collections) were prepared as follows: collagenase type I (120U/ml; Worthington Biochemical, #LS004196) + cycloheximide (CHX; 0.1 mg/ml; Amresco #94217) in 1× Dulbecco modified Eagle medium (DMEM; #31053; Life Technologies); trypsin (50 mg/ml; #LS003708; Worthington) in 10 mM HCl; and DNase I (1 mg/ml; #10104159001; Roche) in 50% glycerol.

1. Testis enzymatic digestion: Testes (mouse) or testes fragments (rat, dog, guinea pig, and mini pig) were placed in 15-ml conical tubes containing 3 ml of DMEM/collagenase I/CHX solution and 10 μl of DNase I solution. The tube was shaken vigorously until the testicular tubules started to disperse and then agitated horizontally at a speed of 120 rpm for 15 min at 33°C. Temperature and agitation speed were the same for all subsequent incubation steps.
2. Somatic cell removal: Tubules were decanted for 1 min vertically at room temperature and the supernatant was discarded to remove somatic cells.
3. Seminiferous tubule digestion: 2.0 ml of DMEM/collagenase I/CHX, 50 μl of trypsin, and 10 μl of DNase I solutions were added and the tube was inverted several times. After a 15-min incubation period, the tubules were gently pipetted up and down for 3 min using a plastic disposable Pasteur pipet with a wide orifice. Then, 30 μl of trypsin and 10 μl of DNase I solution were added and the tube was inverted several times, followed by another 15 min digestion period.
4. Staining with Hoechst: 400 μl of fetal bovine serum (FBS; #10082139; Thermo Scientific) was added and mixed by inverting to inactive trypsin, followed by addition of 5 μl of Hoechst and 10 μl of DNase I. The cell suspension was incubated for 15 min, then passed through two 40-μm 1× DMEM-prewetted disposable filters and stored on ice and protected from light until ready for FACS processing (not more than 30 min).

*Mechanical dissociation of testicular tissue.* Two to three testis fragments of ~2–3 mm$^3$ were placed in a Petri dish containing 100 μl of 1× DMEM, cut with a scalpel, and transferred to a prewetted disposable Medicon disaggregator with 50-μm separator mesh (Cat # 340591; BD Biosciences). Tissue was processed for 5 min and resulting cell suspension was recovered from the Medicon unit with a 3-ml disposable syringe, passed through two 40-μm 1× DMEM-prewetted disposable filters, and transferred back to the Medicon unit for 5 min more of processing. The resulting single cell suspension was transferred to a 1.5-ml tube and stained with 10 μl of Hoechst and 2 μl of PI for 30 min at room temperature in the dark. Samples were then filtered again (40-μm filter) and kept on ice in the dark until FACS processing.

## Fluorescence-Activated Cell Sorting

Cells were sorted and analyzed by a Beckman Coulter MoFlo Legacy cell sorter, using Summit Cell Sorting software, similarly to the descriptions in [8]. Hoechst was excited using a UV laser and triggered for scatter by a 488-nm blue laser. To detect Hoechst's wide emission spectrum, the UV laser was paired with a 463/25-nm band-pass filter for detecting Hoechst blue and a 680-nm LP band-pass filter for Hoechst red. A 555DLP dichroic was also used to distinguish blue from red emission wavelengths. Samples were analyzed using a 70-micron nozzle and the sorting flow rate was set to 1000–2000 events/sec. A minimum of 500 000 events were detected before proceeding to gating. Two different gating strategies were used. For cell suspensions prepared by enzymatic tissue dissociation without PI staining (rat and dog; Supplemental Fig. S1), a sequential cell gating strategy was applied: debris was excluded based on forward scatter (FSC) versus side scatter (SSC) plot, then singlets were gated by adjusting threshold for FSC pulse width, and finally red/blue Hoechst fluorescence was used to detect different spermatogenic germ cell populations. For samples obtained by mechanical dissociation or enzymatic dissociation with PI staining (guinea pig and mini pig) two intermediate gating steps were introduced as previously described by Gaysinskaya and Bortvin [14] for the mouse: debris was excluded based on FSC versus SSC plot, then singlets were gated by adjusting threshold for FSC pulse width. Live single cells, negative for PI, were gated based on PI red fluorescence and FSC and plotted in histograms of cell counts in relation to measurements of Hoechst blue fluorescence. Three peaks with increasing Hoechst fluorescence could be detected representative of haploid (1C), diploid (2C), and tetraploid (4C) cells. This DNA content gate was used to refine populations of spermatocytes (Spc) and Spd, which were then discriminated by finally plotting the function of Hoechst-blue and red fluorescence intensity. Spermatogonial stem cells were identified from PI-negative cells as a direct measurement of Hoechst fluorescence because they represent a side population resulting of Hoechst efflux and therefore Hoechst-blue is not representative of DNA content in these cells. Single stained cell suspensions for Hoechst and PI were used to set optimal photomultiplier tube voltages.

Each testis was processed for 45 min to 1.5 h to collect an average of $6.0 \times 10^6$ cells for each subpopulation. Cells were collected into 1 ml of 1× DMEM + 10% FBS in 5-ml polypropylene round-bottom tubes or 1.5-ml tubes that were precoated with FBS. To concentrate the samples and remove dead cells and cellular debris, sorted cells were pelleted by centrifugation ($600 \times g$ at 4°C for 10 min) and washed in 1 ml of ice-cold 1× PBS.

## Microscopic Evaluation of Purified Cells

To identify the cell types gated in each FACS-sorted population, we evaluated chromatin structure and cell morphology microscopically based on Hoechst fluorescence. During the wash step after FACS, 100 μl of sorted cells was collected, fixed in 4% PFA, and stored at 4°C in the dark. Slides were mounted with 20 μl of fixed cells from each population and visualized in upright confocal or light microscopes. To quantify cell purity, images were obtained from a minimum of 5–15 random fields and/or at least 100 cells (when available) were counted to estimate contamination with other cell types. To avoid human errors, cells were counted independently by two researchers and an estimated average cell count was reported.

## RESULTS

### Efficiency of Tissue Dissociation Protocol Is Crucial for Cell Sorting with Hoechst Staining

We isolated two testes from each animal in the study: 10 mice, 4 rats, 3 dogs, 2 guinea pigs, and 1 mini pig. In order to confirm a normal adult testis phenotype of the collected specimens, we performed HE staining of tissue sections from one testis, and then submitted the other testis for FACS. A microscopy analysis of the HE slides shows the expected tissue architecture and organization of normal adult male testes and highlights some general differences across species (Fig. 1). Mammals have a tubular testicular arrangement, with spermatogenesis progressing from the periphery towards the lumen, and show interspecific variability of germ cell morphology.

The success of cell-sorting protocols depends on the quality of inputted single-cell suspensions, and is therefore directly affected by the efficiency of tissue dissociation. Here, we evaluated the use of different protocols for testis dissociation, enzymatic and mechanical, in each of the species studied. We applied an enzymatic dissociation protocol optimized for mouse testis to all species, referred to as the multispecies protocol, and defined species-specific protocols by adjusting incubation temperatures and times and/or trypsin concentrations and/or introducing the use of hyaluronidase to improve digestion of connective tissues (*Materials and Methods*). To control for technical and biological variables, the experiments were performed simultaneously in tissue sections of the same testis for both biological replicates, except for mini pig. Overall, species-specific dissociation protocols performed better as evaluated by the separation of distinct clusters obtained on the FACS profiles (Supplemental Fig. S1). The main goal of a tissue dissociation protocol is to reduce the amount of manipulation and time while retaining the viability of the dissociated cells. We therefore tested the applicability of mechanical testicular dissociation in different species using a method originally described for rodents [29]. To evaluate the performance of our approach, we estimated the mean percentage of cells that passed the gates during FACS and compared these values with the ones obtained for mouse. The proportion of cells from total counts (Fig. 2) is indicative of the sample quality and a reflection of the efficiency of tissue dissociation protocols. The average percentage of cells passing the debris filter was comparable between species, with mechanical dissociation performing similarly or better when compared to enzymatic dissociation with species-specific protocol. Notably, the percentages estimated for all species
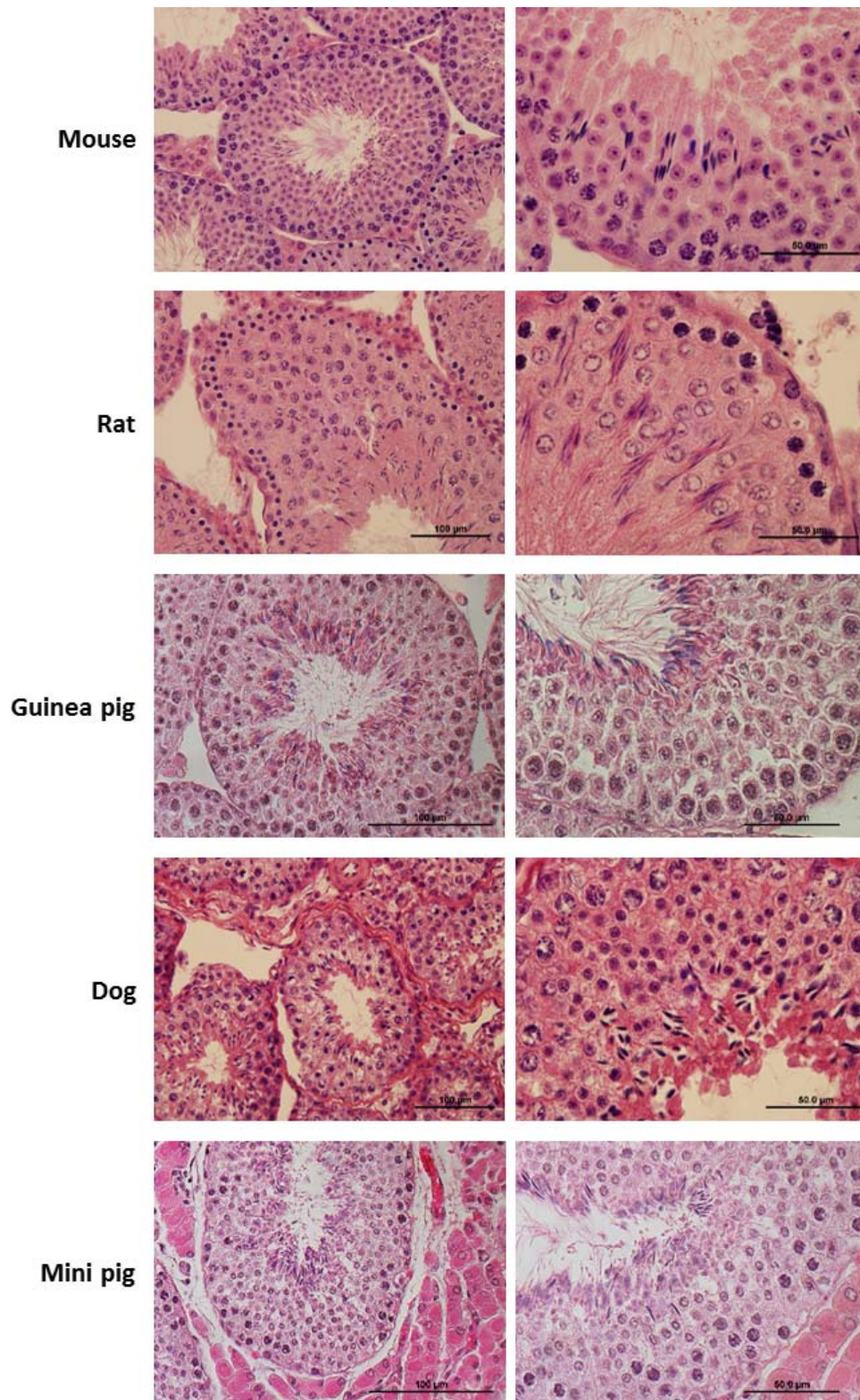
FIG. 1. HE staining of testicular cross sections of collected specimens. For each animal studied in the paper (n = 10 mice, n = 3 dogs, n = 4 rats, n = 2 guinea pigs, n = 1 mini pig) we processed testis fragments for histology and for FACS. Here we present representative HE staining from each species. In each subject, histological examination of testicular cross sections shows the presence of all germ cell types in different developmental stages at lower (left panel) or higher (right panel) magnification, confirming that the specimens were sexually mature and presented a normal testicular phenotype.
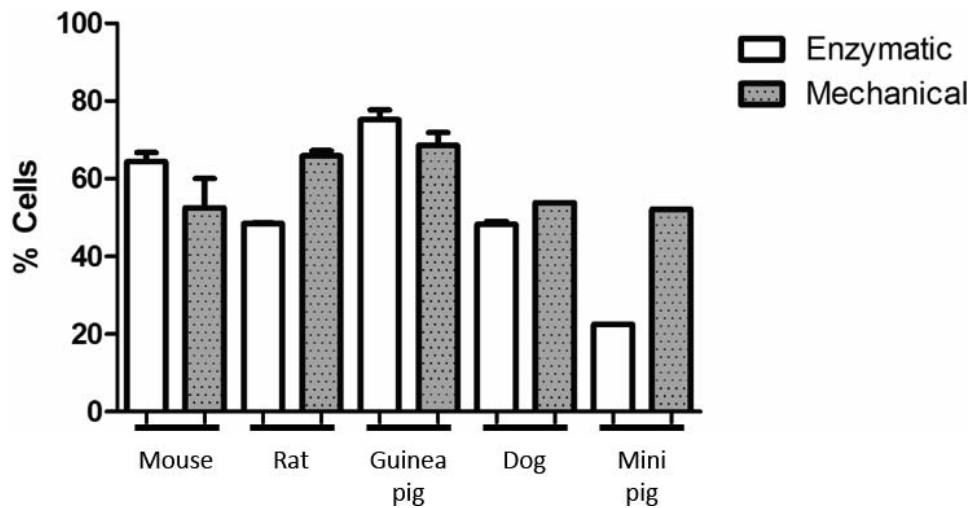
FIG. 2. Evaluation of testis dissociation protocols by flow cytometry. In order to evaluate the efficiency of mechanical and enzymatic dissociation protocols in different species we estimated the percentage of live cells from total number of cells. The quality of mechanical single-cell suspensions was comparable to the species-specific enzymatic dissociation protocol, indicating that this method can be used to quickly obtain single cell suspensions of different mammalian species. Data sets were obtained from variable numbers of experimental replicates (mouse, 10; dog, 3; rat, 4; guinea pig, 2; and mini pig, 1) using FlowJo software v10 (Tree Star Inc.). Histograms were generated with GraphPad Prism (version 5.02 for Windows, GraphPad Software, www. graphpad.com), plotting the calculated mean values with standard deviation.

are directly influenced by the high stringency of the debris filter applied during FACS. These results suggest that cell sorting with Hoechst staining seems very sensitive to sample quality, validating our approach of designing species-specific enzymatic dissociation protocols that are effective in generating good single-cell suspensions. More importantly, mechanical dissociation with Medimachine provides a standard method for testicular dissociation that reduces the processing time and is applicable to different mammalian species.

*Male Germ Cell Types of Different Mammalian Species Can Be Discriminated by Ho-FACS*

We first isolated four different populations (Spg, primary Spc [Spc I], secondary Spc [Spc II], and Spd) from dog and rat testicular cell suspensions obtained from species-specific enzymatic dissociation (Supplemental Fig. S1). The gates for sorting were defined based on the cluster of cells observed and taking into account the expected location of the subpopulations in terms of Hoechst red and blue fluorescence: 1) Spg (side population), low Hoechst blue and red fluorescence; 2) Spc I (4C euchromatin to heterochromatin), high Hoechst blue and a wide range of low to high Hoechst red fluorescence; 3) Spc II (2C euchromatin to heterochromatin), intermediate Hoechst blue and a wide range of low to high Hoechst red fluorescence; 4) Spd (1C compacted chromatin with structural variations resulting from histone to protamine transition), low Hoechst blue and a narrow range of Hoechst red. Moreover, it appears that the chromatin of the dog germ cells is generally more compact throughout spermatogenesis as the clusters of cells show a trend of lower red Hoechst fluorescence. To identify the germ cell types and quantify the purity of the sorted subpopulations, we performed a microscopy evaluation of cell morphology and chromatin structure based on Hoechst fluorescence (*Materials and Methods*). Immunofluorescence in tissue sections with Hoechst was used as reference for the pattern of Hoechst staining in different germ cells (Fig. 3A). Spg are small, round cells with distinct pericentric heterochromatin. Spc are larger

granulated cells, with Spc II populations defined by the detection of binucleated cells or cells in diakinesis. Spd are small 1C cells that can be round or elongated in shape. Despite the similar size, rSpd can be clearly distinguished from Spg by the presence of localized chromocenters. Purity was estimated based on this analysis, indicating 74%–85% purity of specific cell types passing through each gate (Supplemental Table S1) except for the dog Spg population (46%), because of the close proximity of the eSpd and Spg populations in fluorescence space (Supplemental Fig. S1). For the Spc I gates, most contamination was with preleptotene Spc. In the rat, this could have resulted from the absence of clearly defined premeiotic and meiotic Spc subpopulations during FACS.

Then, to ensure the viability of the cells being sorted and to refine the purity of the populations obtained, we applied a gating strategy similar to that described for the mouse in Gaysinskaya et al. [15] (Fig. 4). This strategy includes a viability gate based on PI staining as well as a DNA content gate where a histogram obtained based on Hoechst-blue fluorescence shows peaks representative of 1C, 2C, and 4C cells. Figure 5 shows the cytograms, as a function of Hoechst-blue and red fluorescence, generated during Ho-FACS of single-cell suspensions obtained from testicular tissue of all the different species by mechanical dissociation. Although we see some expected interspecific variation in the pattern of the FACS profiles, we can clearly distinguish at least four subpopulations of male germ cells for all species. The different cell populations were sorted by applying the gating strategy described in Figure 4 and purities were estimated (Table 1) by a similar morphological analysis as described above (Fig. 3). Looking at the relative frequency of cells passing through each gate (Table 1), a similar higher frequency of Spd was detected for all species; however, the abundance of other germ cell types varied among species. These observations were expected and presumably reflect interspecific differences in testis composition and the technical challenge of making standardized settings for subpopulation gating. Interestingly, although this gating strategy generally improved the purity of germ cell
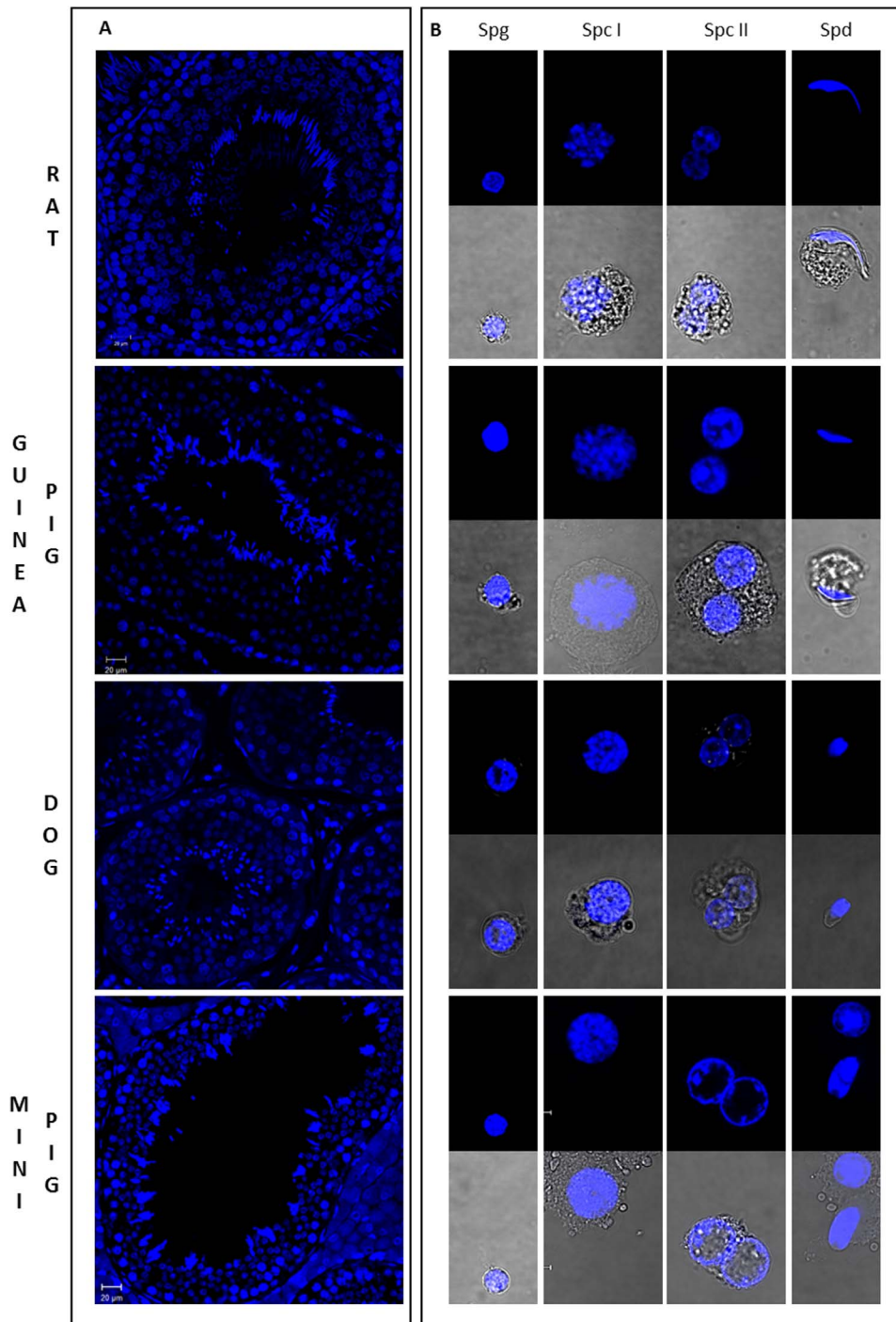
FIG. 3. Microscopic evaluation of germ cell populations isolated from mammalian testes by Ho-FACS. Immunostained cross sections of rat, guinea pig, dog, and mini pig testes (**A**) were used as reference for the classification of isolated germ cells in respect to chromatin structure marked with Hoechst (blue). Morphological evaluation of chromatin structure was performed based on cell shape and size, allowing the identification of different germ cell types (**B**). Spg are small round cells with compact heterochromatin whereas Spc I and Spc II show larger and more complex cells with more diffuse chromatin (Spc I) and/or binucleated cells (Spc II). Spd gates comprise cells in different states of spermiogenesis, ranging from rSpd to completely elongated Spd. Panels indicate the designated FACS gate. Slides were visualized in a confocal microscope. For each isolated population, Hoechst fluorescence of sorted cells was visualized after FACS and images were collected under a ×63 magnification lens, with (lower panel) or without (upper panel) white light transmission.

populations isolated from the rat and dog (Table 1 and Supplemental Table S1), the guinea pig and mini pig Spg populations showed contamination with other cell types and an overall lower level of purity. Altogether, our results suggest that Ho-FACS, combined with PI staining, of testis single-cell suspensions can be used to isolate germ cells from rat, guinea pig, dog, and mini pig, further strengthening our hypothesis that this method can potentially be applied as a generalized procedure for isolation of germ cells in different mammalian species.
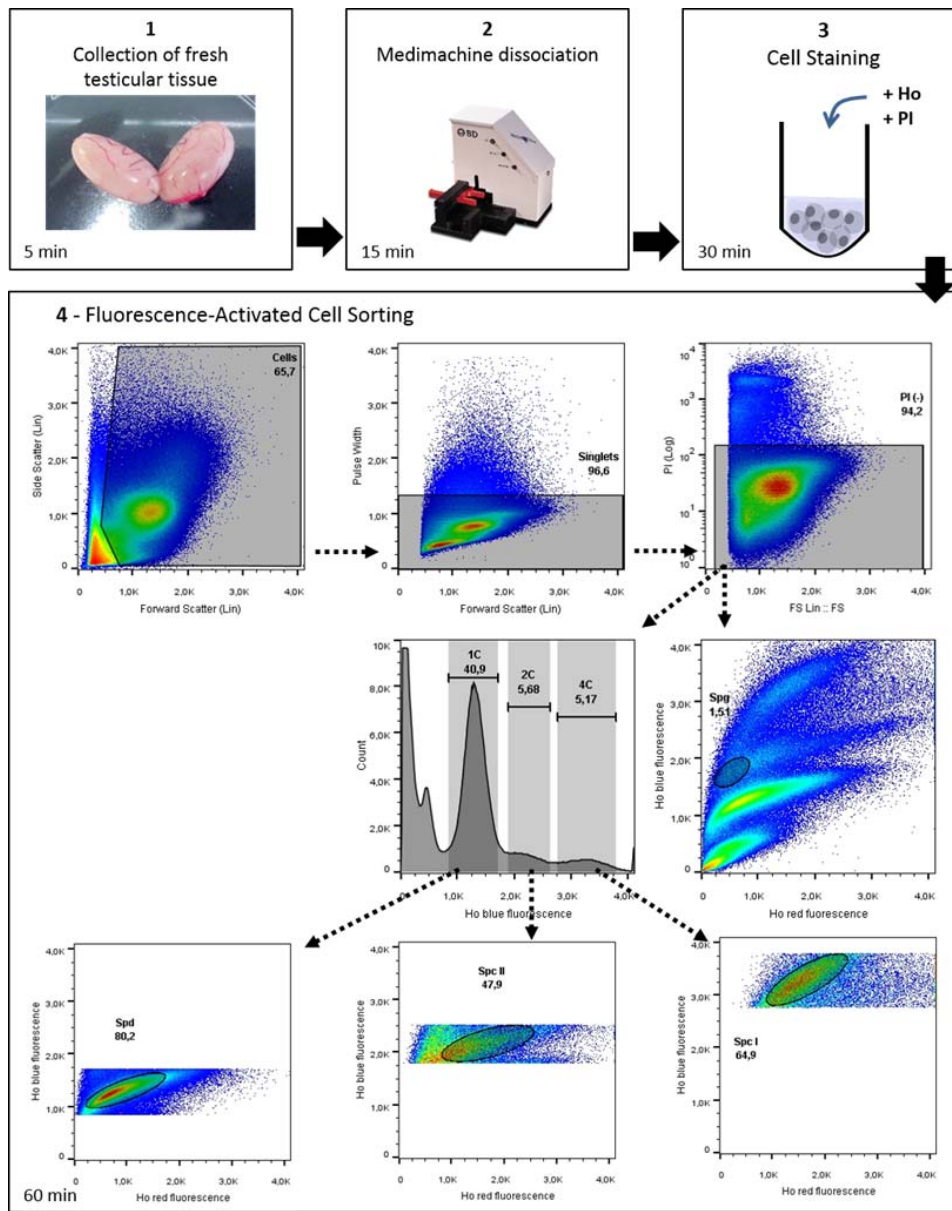
FIG. 4. Workflow of Ho-FACS isolation of mammalian male germ cells. This image summarizes the steps for germ cell isolation of mammalian germ cells, represented here by the application of this protocol to rat testis. The BD Medimachine system is used for mechanical tissue dissociation. FACS is performed in a Beckman Coulter MoFlo Legacy cell sorter (see *Materials and Methods*) and plots generated using FlowJo software v10 (Tree Star Inc.). Ho: Hoechst.

## rSpd and eSpd Can Be Separated by Ho-FACS Based on Cell Shape and Size

During Ho-FACS of the different mammalian species, it was notable that while Hoechst-red and blue fluorescence alone could discriminate rSpd and eSpd populations in the dog sample, it was insufficient to further refine this population in the remaining species (Fig. 5 and Table 1). Given that rSpd and eSpd are molecularly very distinct in terms of transcription activity as well as the differentiation occurring in the latter during spermiogenesis, we sought to evaluate a different strategy to isolate different mouse spermatid subpopulations by FACS. It has been previously suggested that rSpd and eSpd could be gated based on high and low FSC, respectively [13]. Interestingly, we observed that gating based on the FSC parameter alone introduced some contamination in the sorted populations. Microscopy quantification of purity of sorted populations based on cell morphology and Hoechst fluorescence revealed enrichment of ~62% for eSpd and 84% for rSpd (Supplemental Fig. S2). Gating for events with low FSC and high versus low SSC, we increased purity levels to 92% for eSpd and 86% for rSpd (Supplemental Fig. S2). Finally, we observed that the lowest levels of contamination could be obtained by the combination of FSC and SSC gating followed by Hoechst red/blue fluorescence. It seems that eSpd can be isolated gating for low FSC and SSC with 83%–92% enrichment range, whereas rSpd appear to have higher FSC and SSC values and can be separated with 86%–95% accuracy (Fig. 6 and Table 1). Importantly, this gating strategy is based on cell size, shape, and complexity and thus potentially applicable to Ho-FACS of any species undergoing spermiogenesis during gamete development.
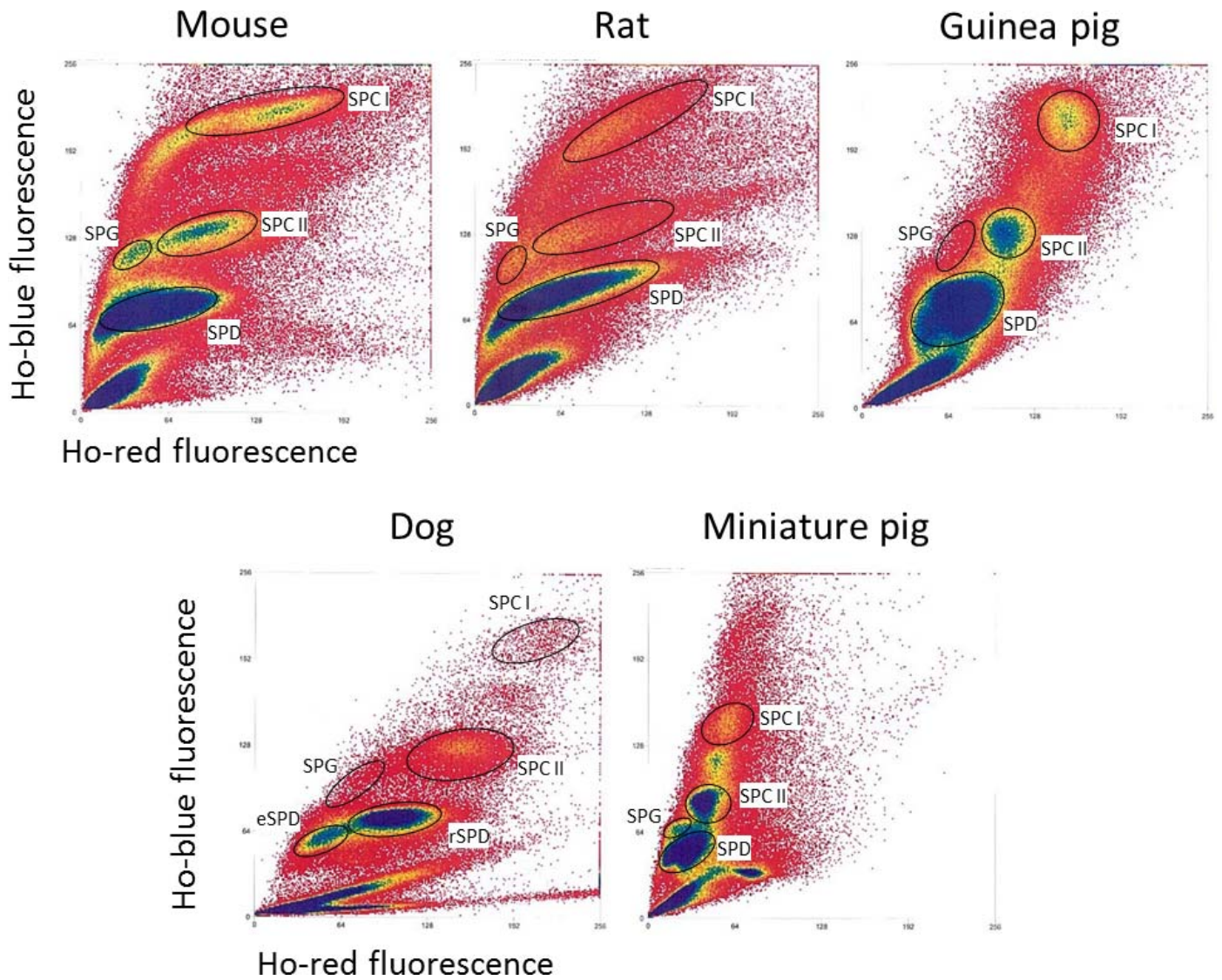
FIG. 5. Interspecific comparison of Ho-FACS plots of testicular single-cell suspensions. The binding of Hoechst to DNA results in different FACS patterns depending on chromatin compaction and quantity. Plots represent the ratio of blue and red Hoechst fluorescence obtained by flow cytometry after testis mechanical dissociation and staining of germ cells of the mouse, rat, guinea pig, dog, and mini pig. Gating (round circles) was defined based on observed cell clusters and expected location of populations in relation to Hoechst fluorescence. A minimum of four populations were identified and sorted for all species. Ho: Hoechst.

## DISCUSSION

One of the major challenges in male reproductive biology has been to design a method to differentiate and isolate subtypes of developing germ cells with a high percentage of recovery and low contamination with other cell types. Since the first reports over a decade ago, flow cytometry of Hoechst-stained murine male germ cells has been slowly revisited and optimized to isolate premeiotic (Spg), meiotic (preleptotene, leptotene, zygotene, pachytene, diplotene, and Spc II) and postmeiotic (rSpd and eSpd) stages [8, 13–16, 32]. This technique is based on measurements of chromatin amount and structure detectable using the fluorescent Hoechst DNA dye. Flow cytometry of testicular cell suspensions from nonmouse

TABLE 1. Statistics of Ho-FACS of male germ cell suspensions obtained by mechanical dissociation.

| Species | Singlets (%) | Live cells (%) | Cells in DNA content gate (%) | | | Purity of sorted germ cell populations (%) | | | | | |
|---|---|---|---|---|---|---|---|---|---|---|---|
| | | | 1C | 2C | 4C | Spg | Spc I | Spc II | Spd | rSpd | eSpd |
| Mouse | 98.4 | 92.5 | 34.7 | 3.9 | 3.72 | 74 | 82 | 87.5 | 95.2 | 95* | 92* |
| Rat | 95.7 | 93.8 | 37.7 | 5.3 | 5.4 | 83 | 81 | 82 | 87 | – | – |
| Guinea pig | 96.2 | 92.1 | 39.3 | 7.6 | 5.8 | 48 | 68.7 | 85 | 87 | – | – |
| Dog | 97.9 | 86.5 | 16.4 | 3 | 0.5 | 78 | – | 87 | – | 91 | 81 |
| Mini pig | 95.9 | 93.2 | 26.9 | 6.4 | 3.5 | 49 | 52 | 82 | 92 | – | – |

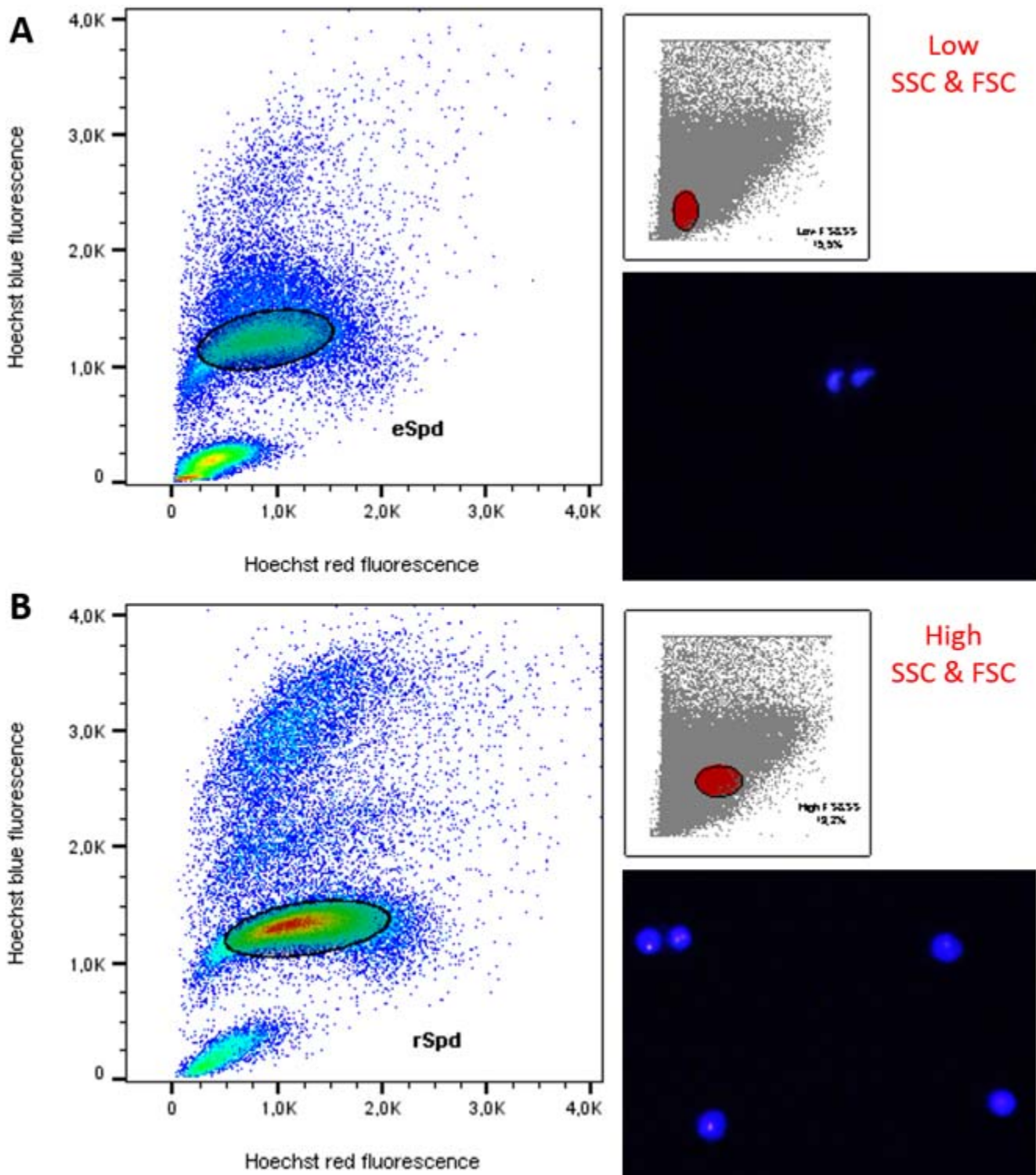* Obtained by enzymatic dissociation and gated based on FSC and SSC parameters (see text).

FIG. 6. Gating strategy to discriminate rSpd and eSpd. Cell shape and complexity influence the ratio of FSC and SSC parameters measured by flow cytometry. The smaller windows in both images show the parent gate (red full circle) based on FSC and SSC. Gated cells then clustered as functions of Hoechst blue/red fluorescence with the pattern expected for 1C cells with condensed chromatin, defining the gates for sorting. Morphology of sorted cells was evaluated microscopically based on Hoechst fluorescence and confirms the enrichment of the expected cell types in each population. Therefore, eSpd are smaller and less complex, showing lower ratios of FSC and SSC (**A**), whereas rSpd present higher FSC and SSC (**B**). Cell images were obtained by light microscopy with a UV lamp (×16 magnification lens). Plots were generated using FlowJo software v10 (Tree Star Inc.).

mammalian species using different dyes, staining protocols, and flow cytometry parameters for analysis has revealed similar profiles in terms of DNA ploidy/stainability (reviewed in [33]). We reasoned that, for species sharing similar

chromatin dynamics (2C-4C-2C-1C) and structure throughout spermatogenesis, major populations of germ cells in different stages could be isolated by Ho-FACS. Here we propose a Ho-FACS standardized protocol for germ cell purification that is

9

fast, straightforward, and applicable to mammalian species beyond the mouse (Fig. 4).

Using three rodent species (mouse, rat, and guinea pig) and two nonrodent species (dog and mini pig), we showed that the general resolution of distinct cell populations is maintained across mammals and allows the isolation of at least four developmental stages: Spg, Spc I, Spc II, and Spd. The purity of these subpopulations was slightly reduced when compared to previous works for the mouse [13, 15], but shows good enrichment of expected cell types (Table 1). It is important to highlight that higher purities of early and mid-late Spc I (93%–97%) have been described for FACS sorting of germ cells with >2 h of PI staining [34], suggesting that longer incubation periods increase the power of discriminating germ cells based on DNA-binding dyes in flow cytometry. Moreover, this could also explain a lower percentage of Spc I cells detected in the guinea pig and rat samples. Nonetheless, a reduced processing time is crucial to preserve the physiology of ex vivo cells and, in that regard, a combination of Hoechst and PI staining for 30 min seems to be sufficient for a good enrichment of different male germ cell types (Fig. 4). The presence of eSpd was the major source of contamination within the Spg gates and resulted from their close special proximity in Hoechst plots, reaching the highest values in the guinea pig and mini pig FACS. One possible way to circumvent this issue would be to stain germ cells with a membrane permeable marker for the acrosome, allowing to gate cells for the presence of this spermatid-specific structure. In fact, Spg is the most challenging population to isolate based on Hoechst staining. Spermatogonial stem cells show a unique Hoechst fluorescence pattern and represent a side population as a result of BCRP1-dependent dye efflux [13]. Other methods such as MACS using Spg-specific markers would be more suitable to isolate spermatogonial stem cells for studies focusing on this particular cell type. Nonetheless, a sample preparation method achieving an enrichment of even 50% Spg is likely to have an important impact as a useful tool in the world of germ cell genomics, especially in single-cell studies.

Future work would also include the optimization of this protocol to discriminate other cell types in different mammals. Here, we describe an optimized gating strategy based on cell size, shape, and complexity to differentiate rSpd and eSpd in the mouse (Fig. 6 and Supplemental Fig. S2), suggesting that the isolation of populations enriched for these germ cells can be achieved for other mammalian species. Also, discrimination between different meiotic stages, already resolved for mouse [13–15], would broaden the scope of the application of this technique in the field of male reproductive biology.

Overall, we provide the first evidence supporting the applicability of Ho-FACS as a transversal method to isolate male germ cells in different developmental stages across mammalian species. As a proof of principle, our work has major implications for several types of studies in developmental biology. First, it provides the tools to investigate the dynamics of germ cell development in different species individually, which would benefit research of understudied mammalian species such as domesticated animals [35]. Furthermore, using the same experimental procedure in different species reduces noise and eliminates sources of variables that often challenge comparative studies. In the ''omics'' era, with the growing interest in applying genome technology to address questions about epigenetics, regulation, and protein diversity throughout spermatogenesis [11, 12, 24–28, 36–39], this technology could be used to comprehensively tackle different aspects of germ cell development with an evolutionary perspective.

## REFERENCES

1. Chen C, Ouyang W, Grigura V, Zhou Q, Carnes K, Lim H, Zhao GQ, Arber S, Kurpios N, Murphy TL, Cheng AM, Hassell JA, et al. ERM is required for transcriptional control of the spermatogonial stem cell niche. Nature 2005; 436:1030–1034.
2. Soumillon M, Necsulea A, Weier M, Brawand D, Zhang X, Gu H, Barthes P, Kokkinaki M, Nef S, Gnirke A, Dym M, de Massy B, et al. Cellular source and mechanisms of high transcriptome complexity in the mammalian testis. Cell Rep 2013; 3:2179–2190.
3. Carelli FN, Hayakawa T, Go Y, Imai H, Warnefors M, Kaessmann H. The life history of retrocopies illuminates the evolution of new mammalian genes. Genome Res 2016; 26:301–314.
4. Good JM, Giger T, Dean MD, Nachman MW. Widespread over-expression of the X chromosome in sterile F(1)hybrid mice. PLoS Genet 2010; 6:e1001148.
5. Rodriguez-Casuriaga R, Folle GA, Santinaque F, Lopez-Carro B, Geisinger A. Simple and efficient technique for the preparation of testicular cell suspensions. J Vis Exp 2013; 78:50102.
6. Bryant JM, Meyer-Ficca ML, Dang VM, Berger SL, Meyer RG. Separation of spermatogenic cell types using STA-PUT velocity sedimentation. J Vis Exp 2013; (80):e50648.
7. Chang YF, Lee-Chang JS, Panneerdoss S, MacLean JA II, Rao MK. Isolation of Sertoli, Leydig, and spermatogenic cells from the mouse testis. Biotechniques 2011; 51:341–342, 344.
8. Getun IV, Torres B, Bois PR. Flow cytometry purification of mouse meiotic cells. J Vis Exp 2011; (50):e2602.
9. Namekawa SH, Park PJ, Zhang LF, Shima JE, McCarrey JR, Griswold MD, Lee JT. Postmeiotic sex chromatin in the male germline of mice. Curr Biol 2006; 16:660–667.
10. Yoshida S, Sukeno M, Nakagawa T, Ohbo K, Nagamatsu G, Suda T, Nabeshima Y. The first round of mouse spermatogenesis is a distinctive program that lacks the self-renewing spermatogonia stage. Development 2006; 133:1495–1505.
11. Laiho A, Kotaja N, Gyenesei A, Sironen A. Transcriptome profiling of the murine testis during the first wave of spermatogenesis. PLoS One 2013; 8: e61558.
12. Margolin G, Khil PP, Kim J, Bellani MA, Camerini-Otero RD. Integrated transcriptome analysis of mouse spermatogenesis. BMC Genomics 2014; 15:39.
13. Bastos H, Lassalle B, Chicheportiche A, Riou L, Testart J, Allemand I, Fouchet P. Flow cytometric characterization of viable meiotic and postmeiotic cells by Hoechst 33342 in mouse spermatogenesis. Cytometry A 2005; 65:40–49.
14. Gaysinskaya V, Bortvin A. Flow cytometry of murine spermatocytes. Curr Protoc Cytom 2015; 72:7.44.1–7.44.24.
15. Gaysinskaya V, Soh IY, van der Heijden GW, Bortvin A. Optimized flow cytometry isolation of murine spermatocytes. Cytometry A 2014; 85: 556–565.
16. Lassalle B, Bastos H, Louis JP, Riou L, Testart J, Dutrillaux B, Fouchet P, Allemand I. ''Side population'' cells in adult mouse testis express Bcrp1 gene and are enriched in spermatogonia and germinal stem cells. Development 2004; 131:479–487.
17. Sandhu LC, Warters RL, Dethlefsen LA. Fluorescence studies of Hoechst 33342 with supercoiled and relaxed plasmid pBR322 DNA. Cytometry 1985; 6:191–194.
18. Watson JV, Nakeff A, Chambers SH, Smith PJ. Flow cytometric fluorescence emission spectrum analysis of Hoechst-33342-stained DNA in chicken thymocytes. Cytometry 1985; 6:310–315.
19. Ellwart JW, Dormer P. Vitality measurement using spectrum shift in Hoechst 33342 stained cells. Cytometry 1990; 11:239–243.
20. Smith PJ, Nakeff A, Watson JV. Flow-cytometric detection of changes in the fluorescence emission spectrum of a vital DNA-specific dye in human tumour cells. Exp Cell Res 1985; 159:37–46.

21. Steen HB, Stokke T. Fluorescence spectra of cells stained with a DNA-specific dye, measured by flow cytometry. Cytometry 1986; 7:104–106.
22. Falciatori I, Borsellino G, Haliassos N, Boitani C, Corallini S, Battistini L, Bernardi G, Stefanini M, Vicini E. Identification and enrichment of spermatogonial stem cells displaying side-population phenotype in immature mouse testis. FASEB J 2004; 18:376–378.
23. Goodell MA, Brose K, Paradis G, Conner AS, Mulligan RC. Isolation and functional properties of murine hematopoietic stem cells that are replicating in vivo. J Exp Med 1996; 183:1797–1806.
24. Liu Y, Niu M, Yao C, Hai Y, Yuan Q, Liu Y, Guo Y, Li Z, He Z. Fractionation of human spermatogenic cells using STA-PUT gravity sedimentation and their miRNA profiling. Sci Rep 2015; 5:8084.
25. McCarrey JR. The epigenome—a family affair. Science 2015; 350: 634–635.
26. Chowdhury R, Bois PR, Feingold E, Sherman SL, Cheung VG. Genetic analysis of variation in human meiotic recombination. PLoS Genet 2009; 5:e1000648.
27. Getun IV, Wu ZK, Khalil AM, Bois PR. Nucleosome occupancy landscape and dynamics at mouse recombination hotspots. EMBO Rep 2010; 11:555–560.
28. Roig I, Dowdle JA, Toth A, de Rooij DG, Jasin M, Keeney S. Mouse TRIP13/PCH2 is required for recombination and normal higher-order chromosome structure during meiosis. PLoS Genet 2010; 6:e1001062.
29. Rodriguez-Casuriaga R, Geisinger A, Lopez-Carro B, Porro V, Wettstein R, Folle GA. Ultra-fast and optimized method for the preparation of rodent testicular cells for flow cytometric analysis. Biol Proced Online 2009; 11: 184–195.
30. Park MH, Park JE, Kim MS, Lee KY, Park HJ, Yun JI, Choi JH, Lee E, Lee ST. Development of a high-yield technique to isolate spermatogonial stem cells from porcine testes. J Assist Reprod Genet 2014; 31:983–991.
31. Reproductive Tissue Dissociation [Internet]. Lakewood, NJ: Worthington Biochemical Corporation. http://www.worthington-biochem.com/tissuedissociation/Reproductive.html. Accessed 29 July 2016.
32. Shimizu Y, Motohashi N, Iseki H, Kunita S, Sugiyama F, Yagami K. A novel subpopulation lacking Oct4 expression in the testicular side population. Int J Mol Med 2006; 17:21–28.
33. Geisinger A, Rodriguez-Casuriaga R. Flow cytometry for gene expression studies in Mammalian spermatogenesis. Cytogenet Genome Res 2010; 128:46–56.
34. Rodriguez-Casuriaga R, Geisinger A, Santinaque FF, Lopez-Carro B, Folle GA. High-purity flow sorting of early meiocytes based on DNA analysis of guinea pig spermatogenic cells. Cytometry A 2011; 79: 625–634.
35. Gonzalez R, Dobrinski I. Beyond the mouse monopoly: studying the male germ line in domestic animal models. ILAR J 2015; 56:83–98.
36. Castaneda J, Genzor P, van der Heijden GW, Sarkeshik A, Yates JR III, Ingolia NT, Bortvin A. Reduced pachytene piRNAs and translation underlie spermiogenic arrest in Maelstrom mutant mice. EMBO J 2014; 33:1999–2019.
37. Gan H, Cai T, Lin X, Wu Y, Wang X, Yang F, Han C. Integrative proteomic and transcriptomic analyses reveal multiple post-transcriptional regulatory mechanisms of mouse spermatogenesis. Mol Cell Proteomics 2013; 12:1144–1157.
38. Rathke C, Baarends WM, Awe S, Renkawitz-Pohl R. Chromatin dynamics during spermiogenesis. Biochim Biophys Acta 2014; 1839:155–168.
39. Schlatt S, Ehmcke J. Regulation of spermatogenesis: an evolutionary biologist's perspective. Semin Cell Dev Biol 2014; 29:2–16.